Chapter 6

Cartilage behaviour modelling

This chapter presents the results of a research activity performed in the Civil and Architectural Engineering Department laboratory of the Technical University of Lisbon under the guidance of Prof. F. Simões.

After having focused on flows in rigid porous media in the previous chapters, let us turn our attention to flows in **deformable** porous media. Hence, this chapter is devoted to the study of cartilage behaviour and the flowing fluids therein. We are interested in developing the equations which govern both the solid and the fluid phases. More precisely, the chemo-hyperelastic material behaviour, the law of mass transfer of exchangeable species between the phases, and the coupled diffusion equations that generalize Darcy's law for seepage flow, Fick's law for ion diffusion and Ohm's law for electrical current flow will be obtained under the continuum model assumption. The theoretical framework of this chapter is based on three articles (6; 57; 58).

An introduction to cartilage histology and the modelling motivations are firstly presented. The framework and hypotheses of the model are then deeper investigated and the governing equations are developed. Electrochemical potentials are introduced and it is shown how Darcy's law can be deduced from basic thermodynamic principles. The solution of the resulting system is explicited and numerical results are compared with experimental measurements from the literature. Finally perspectives are drawn in order to conclude the chapter.

6.1 Introduction

A short introduction to cartilage histology is firstly given in this section. The physiological observations on which the investigated model is based are then presented.

6.1.1 Cartilage histology

In the body function map, the essential role played by articular cartilage is to minimize the friction between the diarthroidal joints covering the long bones. The thickness of a diarthroidal joint is typically 2-4 mm. Cartilage is a soft tissue which, for adult animals and humans, is avascular, aneural and alymphatic. The transport of nutrients toward the cells occurs via the synovial fluid.

Cartilage is mainly made of a collagen fibril net bathed in proteoglycans (PG's) and electrolytes (Fig. 6.1). PG's are large and highly negatively charged molecules. For normal cartilage the negative fixed charge density is 0.1-0.2 mol/l of water. The electrolytes are mainly NaCl and $CaCl_2$ which are dissolved in the water as Na^+ and Ca^{++} cations and Cl^- anions. Water is also present within the infrafibrillar (IF) collagen space and can represent up to 20% to 30% of the cartilage mass. Extrafibrillar (EF) water represents 40% to 60% of the total cartilage weight. Finally collagen represents 50% to 75% of the dry weight of cartilage while proteoglycans represent 15% to 30% of this weight. It is also important to notice that the relative concentrations of these species can vary with depth.

The highly negative charge of PG's makes that they are surrounded by (i) the hydrogen atoms of the water (which is in fact a dipole) and (ii) the ions of the electrolytes which ensure the solution electroneutrality. Absorption of water in the synovial joint results in a swelling of the cartilage, which depends on the PG concentration and the collagen stiffness. Besides, the net charge of the PG's endows them with a repulsive force which allows cartilage to undergo compressive loadings. The elastic Young modulus for normal human cartilage from the femoral head varies from 4-8 MPa in the interior to 1-2 MPa at the surface as the cartilage composition varies with its depth. This repulsive force of the PG's is (i) balanced by the collagen fibrils (and their loading) and (ii) can be shielded by an increased cation concentration[1]. Therefore there is a strong link between the collagen and the PG's. The collagen fibril structure endows cartilage with a differentiated behaviour in tension and compression and with anisotropic properties.

[1] Osteoarthritis (OA) is characterized by a disruption of collagen fibrils and/or weakening of the bonds between collagen and proteoglycans. This makes that the swelling effect by water absorption is less limited. Degradation of collagen stiffness by OA affects both the cartilage tensile and compressive properties.

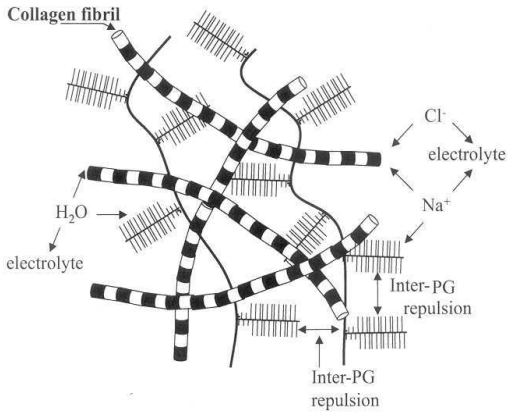

Figure 6.1: Cartilage composition scheme (6) .

Its elastic modulus is indeed higher in tension than in compression. It is also important to note that most collagen fibrils are not electrically charged at the normal human pH (about 7), but this is no longer the case at a pH lower than 5 or higher than 9.5.

Finally, the respective sizes of collagen intrafibrillar space and PG's prevent the latter from flowing inside the fibrils. Nevertheless, this steric effect does not play any preventing role against the anions and cations, which are smaller than the holes between the collagen molecules (Fig. 6.2). The collagen is then acting like a semi-permeable membrane, allowing the small molecules (ions) to penetrate the structure while blocking the large ones (PG's). This is typically the requirement for allowing the osmostic effect to play a role.

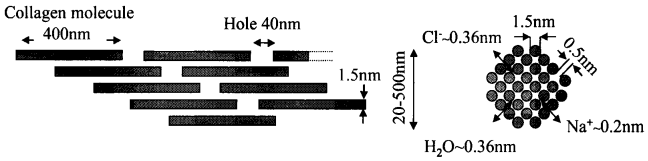

Figure 6.2: Characteristic dimensions of collagen fibers in side view (left) and cross-section (right). Only small molecules, like water and Na^+, can enter the space between the collagen fibrils (6).

From the engineering viewpoint, cartilage is a porous medium bathed in electrolytes

in which electro-chemo-mechanical couplings play a key role. Repulsive forces are generated by the PG charge while collagens keep all the structure together. In addition, the differing collagen and PG geometry is responsible for osmotic effects. Finally, because of the concentration variations of the different molecules, all these properties depend on the location within the cartilage.

6.1.2 Observations of Maroudas and coworkers. Motivations of the model

The intrafibrillar compartment (IFC) is defined as the volume comprised inside the collagen fibrils or more exactly between the collagen molecules. The intrafibrillar compartment is in contact only with the extrafibrillar compartment (EFC), in opposition to the latter which is in contact both with the IFC and with the external water (or synovial fluid). The IFC species can then only be transferred from or to EFC (Fig. 6.3). This separation was shown to be important by Maroudas and coworkers, who indeed proved that the osmotic pressure is almost only influenced by the PG concentration in the EFC. This is why our model must handle the water as separated in two phases, viz. the extrafibrillar and the intrafibrillar phases.

Besides, it is important to observe that there is always a minimum amount of intrafibrillar water, whatever the mechanical and chemical conditions are. Such a mechanism could be due to the so-called **hydration forces**, which act at short distances and are postulated to be the main factor that limits the exchangeability of intrafibrillar water.

To conclude this introductory section, let us qualitatively explain some observations about cartilage behaviour.

- Increasing the bath (or external water) salinity will generate a decrease of the cartilage elastic modulus in compression, as a consequence of the shielding effect of the cations on the PG's.
- Mechanical loading will decrease the water content in the IFC. The loading expels water from EFC, increasing the PG and cation concentrations. This results in a mass transfer of water from IFC to EFC by osmotic effects.
- Decreasing the bath salinity decreases the water content in the IFC. An osmotic pressure due to the presence of PG's in the EFC will indeed be created. Decreasing the salinity will decrease the cation concentration in IFC and EFC. However, this decrease can be lower in the EFC since a minimum number of cations must indeed stay in the EFC. This induces a water transfer from IFC to

EFC. Nevertheless, this phenomenon is stopped when a minimum of IF water is reached.

6.2 Framework and hypothesis of the modelling

This section firstly defines the phases present in the problem. Furthermore, the modelling hypotheses and framework are specified before introducing some notations for the medium geometrical properties and the species concentrations in the different phases.

6.2.1 Definition of the phases

The definition of the phases is mechanically motivated. Therefore, cartilage will be viewed as a three-phase and multi-species porous medium. For the sake of generality, two dissociated salts are considered (NaCl and $CaCl_2$). Three phases are distinguished :

- The solid phase (S) contains the collagens fibers as denoted by the symbol c.
- The intrafibrillar phase (I) contains four species : intrafibrillar water (w), sodium ions (noted Na^+ or Na), calcium ions (noted Ca^{++} or Ca) and chloride ions (noted Cl^- or Cl).
- The extrafibrillar phase (E) contains five species : proteoglycans (PG), water, sodium, calcium and chloride ions.

In this model, the IFC species can only be exchanged with the EFC species. The PG's are only present in the EF phase and the exterior medium only communicates with the extrafibrillar phase (Fig. 6.3).

Let us note that this choice of phases is not unambiguous since a lot of other models exist. Nevertheless, the presented model is devoted to very exactly reproduce the cartilage behaviour and moreover, it is principally based on the observations of Maroudas.

Furthermore attention should be payed to the fact that part of the cations in the EFC is not exchangeable because of the presence of proteoglycans. Nevertheless, although

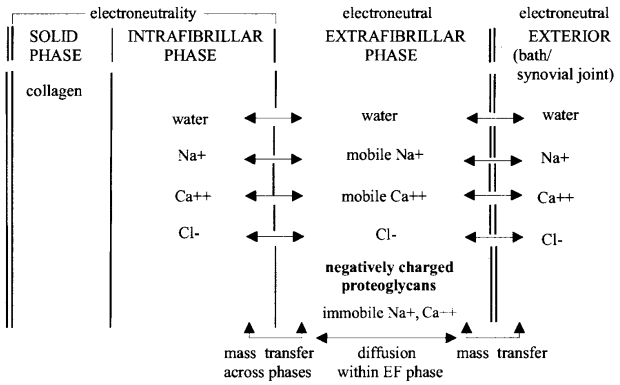

Figure 6.3: Cartilage species partition and exchange schemes (6) .

the specified phases do not consider mobile and non-mobile ions as belonging to different phases, the effect of electroneutrality and diffusion equations will take this phenomenon into account.

We can thus define the following sets :

- $E = \{w, PG, Na, Ca, Cl\}$: set of all species in the extrafibrillar phase
- $E^{mo} = \{w, Na, Ca, Cl\}$: subset of mobile species in EFC.
- $E^{ions} = \{Na, Ca, Cl\}$: subset of ionic species in EFC.
- $I = \{w, Na, Ca, Cl\}$: set of all species in the intrafibrillar phase.
- $I' = \{w, Na, Ca\}$: subset of independent species in I (because of electroneutrality, as it will be further explicited).

6.2.2 Modelling hypotheses

The equations are obtained in a thermodynamical framework following Biot's viewpoint, where the solid is taken as reference. This method considers all the phases and species as a whole. On the contrary, the mixing method considers every phase separately and establishes the complete set of equations for each species in each phase. In

this latter approach a single species is present at any given location, in opposition to the approach of Biot, who considers that there are several species at a given location and is based on a field continuity assumption. After the final averaging required by the mixing method, both approaches lead to a very similar set of equations.

In fact, Biot's approach directly works with the previous averaged variables (the averaging process is included in the continuity assumption of the model). Hence, all the variables are in fact intrinsic phase averages.

The modelling assumptions are the following ones :

(H1) Mass balance is required for each species. The mass balance for each phase is further obtained from the mass balances of the species it contains.

(H2) Momentum balance is required for the mixture as a whole. However, water and ions in the extrafibrillar phase are endowed with their own velocities .

(H3) The velocity of any species in the IF phase is the velocity of the solid phase, i.e. of the collagen ($\underline{v}_s$). Let us note that this assumption does not hinder exchange of water and ions between the two fluid phases, this exchange being viewed as a mass transfer.

(H4) In the IF phase, the pressure in the water and the ionic pressure are assumed to be the same (p_I) while in the EF phase the water and the different ionic species are endowed, through specific constitutive equations, with their own intrinsic pressure.

(H5) Although they are in the EF phase, the proteoglycans move at the same velocity as the solid phase, $\underline{v}_s$.

(H6) Electroneutrality is required both for the EF phase alone, and for the solid and IF fluid phases together.

(H7) All the species are considered as incompressible.

(H8) The problem is isothermal.

(H9) Gravity effects are negligible.

(H10) The analysis of the solid part is restricted to small strains and linear isotropic elasticity.

6.2.3 Notations for geometrical properties and concentrations

Before developing the model, some notations must be introduced and different ways to quantify the species concentrations have to be defined. Finally, some preliminary relations have to be investigated in order to reduce to unknown number.

In the following list, V_0 is the initial volume while V is the current volume. Capital subscripts refer to the phase and non-capital subscripts to species, respectively. Furthermore, $\hat{m}_k$ and M_{kK} represent the molar mass and the mass of species k in phase K, respectively. We can then define :

- $M_k = \sum_K M_{kK}$: the mass of species k [kg],
- $N_{kK} = M_{kK}/\hat{m}_k$: the number of moles of species k in phase K [#mol],
- $m_{kK} = M_{kK}/V_0$: the mass content of species k in phase K [kg/m^3],
- $\rho_{kK} = M_{kK}/V$: the apparent specific mass of species k K [kg/m^3].

Hence, we can infer the following definitions :

- $N_K = \sum_{k\in K} N_{kK}$: the total number of moles in phase K [#mol],
- $\rho_k = M_k/V$: the intrinsic specific mass of species k [kg/m^3],
- $n_{kK} = M_{kK}/M_k$: the mass fraction of species k in phase K [],
- $V_{kK} = VM_{kK}/M_k$: the volume of the species k in the phase K [m^3].

From these definitions, we define :

- $x_{kK} = N_{kK}/N_K$: the molar fraction of species k in phase K [],
- $V_K = \sum_{k\in K} V_{kK}$: the volume of the phase K [m^3],
- $v_{kK} = m_{kK}/\rho_k$: the volume content of species k in phase K [],
- $\hat{v}_k = \hat{m}_k/\rho_k$: the molar volume of species k [m^3],

and finally :

- $c_{kK} = N_{kK}/V_K$: the molar concentration of the species k in phase K [#mol/m^3],
- $\hat{v}_K = V_K/N_K$: the molar volume of phase K [m^3/mol].

These quantities are linked together by numerous relations among which :

- $\sum_{k\in K} x_{kK} = 1$,
- $\sum_K V_{kK} = V$,
- $\hat{v}_K = \sum_k x_{kK}\hat{v}_k$,
- $\rho_k = M_{kK}/V_{kK}$,
- $\rho_{kK} = n_{kK}\rho_k$,
- $n_{kK} = V_{kK}/V$,
- $v_{kK} = V_{kK}/V_0 = n_{kK}V/V_0$,
- $m_{kK} = \rho_k v_{kK}$,
- $N_{kK}/V_0 = m_{kK}/\hat{m}_k$,
- $c_{kE} = \frac{N_{kE}}{V_E} = \frac{N_{kE}}{N_E\hat{v}_E} = \frac{V_{kE}}{\hat{v}_k V_E} = \frac{n_{kE}}{\hat{v}_k n_E} = \frac{v_{kE}V_0}{\hat{v}_k n_E V} = \frac{m_{kE}V_0}{\hat{m}_k n_E V} = \frac{x_{kE}}{\hat{v}_E}, k \in E$.

All these relations will be useful for the next developments. Particularly, the last relations show that molar fractions can be expressed in terms of mass contents. The latter will indeed be taken as primary variables in our formulation.

Before developing conservation equations, let us first investigate some consequences of electroneutrality and incompressibility and show how the number of unknowns of the problem can be reduced. Some previous developments will thus be detailed. The partition of the extrafibrillar compartment will also be commented.

Link between ion masses : electroneutrality

The electroneutrality (H6) fulfillment means that the total electric density in any given phase is constrained to vanish. Let us denote the electric density of phase K by I_{eK} [C/m^3]. Only the ions and proteoglycans can generate a non-vanishing density

charge, while the latter can be expressed as a function of the ion valences (ζ_k) and mole numbers (N_{kK}). Electric density is then written as :

$$I_{eK} = \frac{F}{V}\sum_{k\in K}\zeta_k N_{kK} = F\frac{V_0}{V}\sum_{k\in K}\zeta_k\frac{m_{kK}}{\hat{m}_k}, \tag{6.2.1}$$

where F is the Faraday constant[2]. The electroneutrality fulfillment implies that $I_{eK} = 0$, or equivalently that

$$\sum_{k\in K}\zeta_k\frac{m_{kK}}{\hat{m}_k} = \frac{m_{NaK}}{\hat{m}_{Na}} + 2\frac{m_{CaK}}{\hat{m}_{Ca}} - \frac{m_{ClK}}{\hat{m}_{Cl}} + \zeta_{PG}\frac{m_{PGK}}{\hat{m}_{PG}} = 0 \quad K = I,E. \tag{6.2.2}$$

Let us here note that $m_{PGI} = 0$ as the proteoglycans are only present in the EFC. The anion chloride mass contents is thus directly function of the cation mass contents and, for the EF phase, of the proteoglycan mass content, which provides :

$$\frac{m_{ClK}}{\hat{m}_{Cl}} = \frac{m_{NaK}}{\hat{m}_{Na}} + 2\frac{m_{CaK}}{\hat{m}_{Ca}} + \zeta_{PG}\frac{m_{PGK}}{\hat{m}_{PG}} \quad K = I,E. \tag{6.2.3}$$

The electroneutrality principle is obviously respected in the beginning but also during the remaining of the process. Mole changes are then linked in such a way that electroneutrality remains verified, which is written as :

$$-\delta N_{ClK} + \delta N_{NaK} + 2\delta N_{CaK} = 0 \quad K = I,E. \tag{6.2.4}$$

Let us remark that, since the PG mole number is fixed, it does not have any influence in these variation equations. The chloride content variations are then only determined by the cation content variations :

$$\delta N_{ClK} = \delta N_{NaK} + 2\delta N_{CaK} \quad \Longleftrightarrow \quad \frac{\delta m_{ClK}}{\hat{m}_{Cl}} = \frac{\delta m_{NaK}}{\hat{m}_{Na}} + 2\frac{\delta m_{CaK}}{\hat{m}_{Ca}}, \quad K = I,E. \tag{6.2.5}$$

Because of the presence of the PG's a minimum amount of cations is always required in the EFC :

$$\sum_{k\in E}\zeta_k N^{nm}_{kE} = N^{nm}_{NaE} + 2N^{nm}_{CaE} + \zeta_{PG}N_{PG} = 0 \quad \Longleftrightarrow \quad \sum_{k\in E}\zeta_k\frac{m^{nm}_{kE}}{\hat{m}_k} = 0. \tag{6.2.6}$$

The superscript *nm* means that these ions are "no-mobile" in the sense that a minimum number of cations should always be present in the extrafibrillar phase. Even if the number of PG moles is quite low and negligible, its product with the PG valence cannot be neglected. The presence of the proteoglycans thus constrains some cations to be fixed.

In every case, it appears that the anion masses are linked to the cation masses by Eq. (6.2.3) and determined by it. Hence these relations will be inserted in the following developments. The anion mass contents are then taken into account even if not explicitly appearing in the equations.

[2] F is the charge per electron mole (96368 C/mol).

Link between relative volume changes of the solid and the fluid phases : fluid incompressibility

When all the species are incompressible, that is $\delta\rho_k = 0, \forall k$, the relative volume change of the solid part, i.e. $\mathrm{tr}\,\underline{\underline{\varepsilon}}$, must be the same as the relative volume change of the fluid. For phase K, the latter is equal to :

$$\delta v_K = \frac{\delta m_{wK}}{\rho_w} + \frac{\delta m_{NaK}}{\rho_{Na}} + \frac{\delta m_{CaK}}{\rho_{Ca}} + \frac{\delta m_{ClK}}{\rho_{Cl}} = \frac{\delta m_{wK}}{\rho_w} + \frac{\delta m_{NaK}}{\rho_{s1}} + \frac{\delta m_{CaK}}{\rho_{s2}}, \quad (6.2.7)$$

where the salt specific masses are defined as :

$$\frac{1}{\rho_{s1}} = \frac{1}{\rho_{Na}} + \frac{\hat{m}_{Cl}}{\hat{m}_{Na}}\frac{1}{\rho_{Cl}} \quad \text{and} \quad \frac{1}{\rho_{s2}} = \frac{1}{\rho_{Ca}} + 2\frac{\hat{m}_{Cl}}{\hat{m}_{Ca}}\frac{1}{\rho_{Cl}}. \quad (6.2.8)$$

The incompressibility condition is then finally expressed as :

$$\mathrm{tr}\,\underline{\underline{\varepsilon}} = \delta v_I + \delta v_E. \quad (6.2.9)$$

6.3 Balance equations

In this section, the mass and momentum balance equations are developed.

6.3.1 Mass balance

As expressed by hypothesis (H1), verifying mass balance for every species is required. The species concentration change at a given spatial point can be governed by two mechanisms : a phase transformation or simple transport. These two mechanisms will be called **transfer** and **transport**[3].

In order to establish a rule describing the mass content evolution with respect to the solid phase, we consider that matter motion is relative to the solid phase, which moves at the velocity $\underline{v}_s$. Since the intrafibrillar phase moves together with the solid phase, there is no transport phenomenon in this compartment, for any species. Accordingly, the IF species mass content can only be modified by phase transformations. On the contrary, in the EF phase each species experiences its own velocity. Matter can then be transferred to or from the outside of this phase or transported inside this phase. Then,

[3] In (6), the "transport" mechanism is called "diffusion".

noting the time derivative with respect to the solid phase as $\frac{D^s.}{Dt}$, the rate of transfer of the considered species as $\dot{\rho}^{kK}$ [kg/m^{3}s] and the outgoing mass flux as $\underline{M}_{kE}$ [kg/m^{2}s], previous considerations provide :

$$\begin{array}{rcl} \frac{D^s m_{kI}}{Dt} & = & \dot{\rho}^{kI} \\ \frac{D^s m_{kE}}{Dt} & = & \dot{\rho}^{kE} - \underline{\nabla} \cdot \underline{M}_{kE}, \end{array} \tag{6.3.10}$$

where $\underline{M}_{kE}$ is defined as :

$$\underline{M}_{kE}/\rho_k = \underline{J}_{kE} = n_{kK}^{mo} \left(\underline{v}_{kE} - \underline{v}_S \right) , \tag{6.3.11}$$

where the superscript *mo* refers to the '*mobile*' ions, which are not constrained to remain around the proteoglycans. Furthermore, the matter created in one phase must disappear in the other phase, which is written as :

$$\dot{\rho}^{kI} + \dot{\rho}^{kE} = 0 . \tag{6.3.12}$$

Introducing Eq. (6.3.12) into Eq. (6.3.10) provides :

$$\frac{D^s v_{kE}}{Dt} = -\frac{D^s v_{kI}}{Dt} - \underline{\nabla} \cdot \underline{J}_{kE}, \quad \forall k \in E . \tag{6.3.13}$$

In order to illustrate the effects of these laws, let us analyze the consequences of the incompressibility constraint. The rate of relative volume change of the solid part ($\underline{\nabla} \cdot \underline{v}_s$) is the opposite of the volumic outgoing flux from the extrafibrillar part. Indeed, there is no transfer phenomenon between bath and EFC and the transfers between EFC and IFC are equilibrated. Defining the extrafibrillar outgoing volume flux as $J_E = \sum_{k \in E} M_{kE}/\rho_k = \sum_{k \in E} J_{kE}$, these considerations then provide the relation :

$$\underline{\nabla} \cdot \underline{v}_s + \underline{\nabla} \cdot \underline{J}_E = 0, \tag{6.3.14}$$

6.3.2 Momentum balance

Considering hypothesis (H2), momentum balance has to be imposed to the mixture as a whole. Under quasi-static loading and with gravity as the sole body force, momentum balance writes as :

$$\underline{\nabla} \cdot \underline{\sigma} + \rho \underline{g} = 0, \tag{6.3.15}$$

where ρ is the density of the porous medium, i.e. $\rho = \sum_{k,K} \rho_{kK} = \sum_{k,K} M_{kK}/V$.

6.4 Clausius-Duhem inequality and constitutive equations. Problem closure

In this section, the Clausius-Duhem inequality is first presented in the framework of our specific study. It is important to remind that this inequality plays a key role in Thermodynamics since it is used to develop thermodynamically correct constitutive equations. This is illustrated in this section in order to generate (i) chemo-hyperelastic constitutive equations, (ii) a transfer law of exchangeable species between the IF and EF phases and (iii) coupled diffusion equations to generalize Darcy's law of seepage flow through the porous medium, Fick's law of ion diffusion in the extrafibrillar phase, and Ohm's law of electrical current flow. It is further shown that these additional equations close up the equation set by completing the unknowns and the related equations. Finally some model improvements are suggested.

Let us first recall that the Clausius-Duhem inequality takes into account the total dissipation occurring in the observed medium. It can be shown that **for porous media saturated with reactive fluids in the isothermal case**, the Clausius Duhem inequality writes as (59):

$$-\frac{D^s\psi}{Dt}+\underline{\underline{\sigma}}:\frac{D^s\underline{\underline{\varepsilon}}}{Dt}-\sum_{k,K}\underline{\nabla}\cdot(\mu^{ec}_{kK}\underline{M}_{kK})\geq 0, \tag{6.4.16}$$

where ψ is the volumic Helmotz free energy [J/m^3], $\underline{M}_{kK}$ is the relative mass flux [kg/m^{2}s] and μ^{ec}_{kK} is the electro-chemical potential [J/kg] of species k in phase K. This potential is classically defined as the electro-chemical Gibbs potential and takes into account electrical (ϕ^K), chemical (x_{kK}) and general pressure (p_{kK}) effects. Its definition is therefore composed of three terms :

$$\mu^{ec}_{kK}=\frac{p_{kK}}{\rho_k}+\frac{RT}{\hat{m}_k}\ln x_{kK}+\frac{\zeta_k F}{\hat{m}_k}\phi^K\ , \tag{6.4.17}$$

where ϕ^K is the electrical potential in phase K, ζ_k is the k-species valence and R is the universal gas constant (8.3145 J/mol°K). The chemical activities have been taken equal to one and the species are assumed to be incompressible.

Developing the divergence term of Eq. (6.4.16), and introducing the mass conservation law (6.3.10) this relation transforms into :

$$\underbrace{-\frac{D^s\psi}{Dt}+\underline{\underline{\sigma}}:\frac{D^s\underline{\underline{\varepsilon}}}{Dt}-\sum_{k,K}\frac{D^s m_{kK}}{Dt}\mu^{ec}_{kK}}_{\frac{D^sD_1}{Dt}}\underbrace{-\sum_{k,K}\dot{\rho}^{kK}\mu^{ec}_{kK}}_{\frac{D^sD_2}{Dt}}\underbrace{-\sum_{k,K}\underline{\nabla}\mu^{ec}_{kK}\cdot\underline{M}_{kK}}_{\frac{D^sD_3}{Dt}}\geq 0. \tag{6.4.18}$$

This inequality can be viewed as composed of three terms[4], viz. from left to right :

- the intrinsic dissipation, so-called because of its dependence upon the state variables ;
- the dissipation associated to the mass transfer between the phases ;
- and the dissipation associated to the fluid mass transport.

As previously written, the sum of these terms is the total dissipation, also called the **electro-chemo-mechanical** dissipation[5].

To verify inequality (6.4.18) we will impose a **sufficient** condition, in the sense that each of the three terms will be imposed as non-negative :

$$\left\{\begin{array}{lcl} \frac{D^s D_1}{Dt} & = & -\frac{D^s \psi}{Dt} + \underline{\underline{\sigma}} : \frac{D^s \underline{\underline{\varepsilon}}}{Dt} + \sum_{k,K} \mu^{ec}_{kK} \frac{D^s m_{kK}}{Dt} \geq 0 \\ \frac{D^s D_2}{Dt} & = & -\sum_{k\in I} \left(\mu^{ec}_{kI} - \mu^{ec}_{kE}\right) \frac{D^s m_{kI}}{Dt} \geq 0 \\ \frac{D^s D_3}{Dt} & = & -\sum_{k\in E^{mo}} \underline{\nabla} \mu^{ec}_{kE} \cdot \underline{M}_{kE} \geq 0 \, . \end{array}\right. \tag{6.4.19}$$

In the latter formulation, the summation sets in D_2 and D_3 have been changed, considering that the mass transfers are equilibrated (6.3.12) and that the mass fluxes of intrafibrillar ions with respect to the solid phase are equal to zero.

The first term will exactly vanish and lead to the chemo-hyperelastic constitutive equations. From the second term, we will obtain the transfer law of exchangeable species between the IF and EF phases, while the last term will generate coupled diffusion equations that generalize Darcy's law of seepage flow through the porous medium, Fick's law of diffusion of ions in the extrafibrillar phase and Ohm's law of electrical current flow.

Finally, defining the chemical potentials of the dissociated salts as :

$$\mu_{s1K} = \frac{\hat{m}_{Na}\mu^{ec}_{NaK} + \hat{m}_{Cl}\mu^{ec}_{ClK}}{\hat{m}_{Na}} \quad \text{and} \quad \mu_{s2K} = \frac{\hat{m}_{Ca}\mu^{ec}_{CaK} + 2\hat{m}_{Cl}\mu^{ec}_{ClK}}{\hat{m}_{Ca}} \, , \tag{6.4.20}$$

and using the electroneutrality conditions of the extrafibrillar phase alone and of the solid and intrafibrillar phase together Eq. (6.2.5), the first inequality of Eq. (6.4.19)

[4] In a thermal problem, there will be one additional term, viz. the conduction dissipation term.

[5] In the non-isothermal case, the total dissipation is composed of heat conduction and of electro-chemo-mechanical dissipation effects.

provides the incremental free energy :

$$\delta\psi = \underline{\sigma} : \delta\underline{\varepsilon} + \mu_{wI}\delta m_{wI} + \mu_{s1I}\delta m_{NaI} + \mu_{s2I}\delta m_{CaI} + \mu_{wE}\delta m_{wE} + \mu_{s1E}\delta m_{NaE} + \mu_{s2E}\delta m_{CaE}. \tag{6.4.21}$$

and hence it is also possible to rewrite the second inequality of (6.4.19) as :

$$\frac{D^s D_2}{Dt} = -\left(\mu_{wI} - \mu_{wE}\right)\frac{D^s m_{wI}}{Dt} - \left(\mu_{s1I} - \mu_{s1E}\right)\frac{D^s m_{NaI}}{Dt} - \left(\mu_{s2I} - \mu_{s2E}\right)\frac{D^s m_{CaI}}{Dt} \geq 0. \tag{6.4.22}$$

6.4.1 Helmotz free energy : chemical potential, stress and homogeneous problem closure

In this section, a first illustration of the power of the second principle inequality will be provided. The constitutive equations will indeed be derived as resulting from formulation (6.4.19). Furthermore, it will be shown that, in the **homogeneous equilibrium** case, the equation set is complete and that the elastic problem can therefore be solved.

To introduce this section, let us first recall the local state postulate (59). It stipulates that any state of a homogeneous system[6] undergoing any possible evolution can be characterized by the same constitutive variables as at equilibrium, and is independent of the evolution rate. Characterizing a system means determining its internal energy state, not including its kinetic energy.

Hence, considering the previous postulate, the system Helmotz free energy (ψ) is expressed as a function of deformation $\underline{\varepsilon}$ and mass contents m_{kK} only, which writes as

$$\psi = \psi\left(\underline{\varepsilon}, m_{kK}\right) . \tag{6.4.23}$$

This free energy can be viewed as composed of a purely chemical, a mechanico-chemical and a configurational part (6). We will ensure that the first inequality of (6.4.19) is respected by imposing that the left expression is equal to zero, which provides the equality :

$$\frac{D^s\psi}{Dt} = \underline{\sigma} : \frac{D^s\underline{\varepsilon}}{Dt} + \sum_{k,K}\mu^{ec}_{kK}\frac{D^s m_{kK}}{Dt}. \tag{6.4.24}$$

In order to verify this equation, postulate (6.4.23) implies two (the two first) constitutive equations, viz. :

$$\frac{\partial\psi}{\partial\underline{\varepsilon}} = \underline{\sigma} \quad \text{and} \quad \frac{\partial\psi}{\partial m_{kK}} = \mu^{ec}_{kK}. \tag{6.4.25}$$

[6] A homogeneous system can be a subsystem of a continua medium system.

After some developments (60), the latter equations provide then the constitutive equations

- for the stress tensor :

$$\underline{\sigma} = -p^{eff}\,\underline{\delta} + \underline{\underline{E}} : \underline{\varepsilon}\,, \tag{6.4.26}$$

where $\underline{\underline{E}}$ is the fourth order elasticity tensor[7]. As it can be observed, the elastic moduli vary with the bath salinity (Fig. 6.4). The Lamé parameters of $\underline{\underline{E}}$ are determined in the **hypertonic state**, which is defined as the state of maximum salinity of the extrafibrillar compartment. In this case the salt shielding effect is maximum and the proteoglycans have a very small mechanical effect. In the hypertonic configuration, the stress is then equal to the bath pressure, and by convention, the strain is equal to zero.

Defining the **effective stress** as $\tilde{\underline{\sigma}} = \underline{\sigma} + \underline{\delta} p^{eff}$ highlights the contribution of the effective pressure. Indeed, with the help of this definition, the linear elastic stress law is recovered[8] since Eq. (6.4.26) then provides the relation :

$$\tilde{\underline{\sigma}} = \underline{\underline{E}} : \underline{\varepsilon}\,. \tag{6.4.28}$$

The effective pressure term takes into account the shielding effect in the stifness of the cartilage and the following form was suggested in [9] (6) :

$$p^{eff}(m_{NaE}, \operatorname{tr}\underline{\varepsilon}, p_B) = \Lambda(m_{NaE})\left((\operatorname{tr}\underline{\varepsilon}^I - \operatorname{tr}\underline{\varepsilon}) + p_B \operatorname{tr}\underline{\varepsilon}^I = \left(1 - \frac{\operatorname{tr}\underline{\varepsilon}}{\operatorname{tr}\underline{\varepsilon}^I}\right) p_0^{eff}(m_{NaE}) + p_B\,, \tag{6.4.29}$$

where p_0^{eff} represents the PG effect when a zero displacement is imposed while the bath salinity can be changed (Fig. 6.4). The expression of p_0^{eff} is one of the lacking constitutive equations. Loret et al. (6) nevertheless suggest an interpolation formulation of p_0^{eff}, considering two extreme cases, viz. the cartilage is either in the hypertonic state or bathed in distilled water. Fig. 6.4 highlights the PG influence. Indeed typically, at a constant strain, an increase of the bath salinity will reduce the stress, this effect being attributed to an increased shielding

[7] The collagen fibers endow the cartilage with a differential behaviour in tension and compression. Such a behaviour is known as conewise strain-based. The model can take this effect into account by means of the parameters defining the elasticity tensor, viz. the Lamé coefficients (λ and μ). It can be shown that the continuity stress requirement implies then that only the first Lamé coefficient can vary across the hyperplane $\operatorname{tr}\underline{\varepsilon} = 0$ (with $\otimes$ and $\boxtimes$ denoting appropriate tensorial operators) :

$$\begin{array}{ll} \underline{\underline{E}}^- = \lambda^- \underline{\delta} \otimes \underline{\delta} + 2\mu\, \underline{\delta} \boxtimes \underline{\delta}, & \text{if} \quad \operatorname{tr}\underline{\varepsilon} \le 0 \\ \underline{\underline{E}}^+ = \lambda^+ \underline{\delta} \otimes \underline{\delta} + 2\mu\, \underline{\delta} \boxtimes \underline{\delta}, & \text{if} \quad \operatorname{tr}\underline{\varepsilon} \ge 0 \end{array} \tag{6.4.27}$$

[8] In the same way as in soil mechanics, this principle derives from the well-known *Terzaghi's assumption*, which states that for an incompressible matrix phase and an isotropic saturated porous medium, the linear elastic stress law is recovered when the included pore fluid pressure is in the stress term.

[9] The function is here given for a single salt. An appropriate formulation of p^{eff} for two salts can be found in (57).

of the charged proteoglycans by the dissolved salts. Nevertheless, p^{eff} is still positive in order to take into account the repulsive effect of the proteoglycans. Finally in Eq. (6.4.29) $\underline{\varepsilon}^I$ is defined as the fictitious intersection point of the lines for different salinities in a strain-stress diagram.

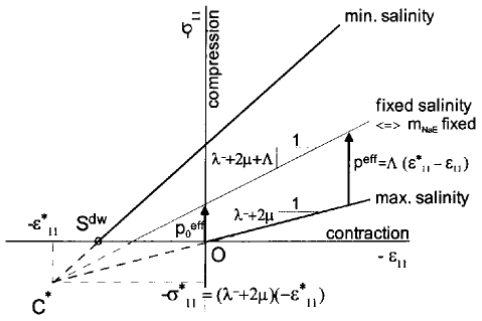

Figure 6.4: Definition of ε_I. Definition and meaning of p^{eff} as function of the salinity.

- for the electro-chemical potentials in extrafibrillar and intrafibrillar phases :

$$\left\{\begin{array}{lcl} \mu_{wE} & = & \frac{p_I+p_w^{cf}}{\rho_w}+\frac{RT}{\hat{m}_w}\ln x_{wE} \\ \mu_{NaE}^{ec} & = & \frac{p_{Na}^{cf}}{\rho_{Na}}+\frac{RT}{\hat{m}_{Na}}\ln x_{NaE}+\frac{\zeta_{Na}F\phi^E}{\hat{m}_{Na}} \\ \mu_{CaE}^{ec} & = & \frac{p_{Ca}^{cf}}{\rho_{Ca}}+\frac{RT}{\hat{m}_{Ca}}\ln x_{CaE}+\frac{\zeta_{Ca}F\phi^E}{\hat{m}_{Ca}} \\ \mu_{ClE}^{ec} & = & \frac{p_{Cl}^{cf}}{\rho_{Cl}}+\frac{RT}{\hat{m}_{Cl}}\ln x_{ClE}+\frac{\zeta_{Cl}F\phi^E}{\hat{m}_{Cl}}\ , \end{array}\right. \qquad \left\{\begin{array}{lcl} \mu_{wI} & = & \frac{p_I+p^h}{\rho_w}+\frac{RT}{\hat{m}_w}\ln x_{wI} \\ \mu_{NaI}^{ec} & = & \frac{RT}{\hat{m}_{Na}}\ln x_{NaI}+\frac{\zeta_{Na}F\phi^I}{\hat{m}_{Na}} \\ \mu_{CaI}^{ec} & = & \frac{RT}{\hat{m}_{Ca}}\ln x_{CaI}+\frac{\zeta_{Ca}F\phi^I}{\hat{m}_{Ca}} \\ \mu_{ClI}^{ec} & = & \frac{RT}{\hat{m}_{Cl}}\ln x_{ClI}+\frac{\zeta_{Cl}F\phi^I}{\hat{m}_{Cl}}\ . \end{array}\right. \tag{6.4.30}$$

The role of pressure in the (electro-)chemical potential has to be commented. The observations of Maroudas and coworkers indeed highlight the different roles of the extrafibrillar and intrafibrillar compartments. In particular, these authors show the key role of the PG's and the extrafibrillar components. Hence, in order to take into account the cartilage history, a configurational energy term[10] is introduced in the extrafibrillar potential (p_k^{cf}/ρ_k).

[10]This term can be determined by solving equilibrium laws in the case of a single salt (6). If several salts are present, the determination of p_k^{cf} depends on the initial salt repartition.

In order to assure that there is always a minimum amount of water in the IF space, as the experimental results seem to indicate, a constitutive function (p^h) was introduced in the electro-chemical potential of the IF water. This function depends on the IF water mass content and was modeled in (6) by an interpolating function between the two limit cases: cartilage in the hypertonic state or bathed in distilled water.

A last remark about the form of the electro-chemical potentials is required in order to highlight the respective roles of mechanical and chemical effects. The molar fraction of a salt is usually by far smaller than unity ($x_{NaK} \ll 1$, $x_{CaK} \ll 1$ and $x_{ClK} \ll 1$). The logarithmic term is therefore dominant in expressions (6.4.31) and (6.4.30) and in a first approximation the pressure term due to mechanical effect in the salt potential has then been neglected in front of the chemical term. In the case of water as a species, the inverse effect is however observed. Since $x_{wK} \approx 1$, the mechanical term is indeed higher than the chemical term.

Using the definitions (6.4.20), the potentials of dissociated salts are rewritten as :

$$\left\{\begin{array}{lcl} \mu_{s1E} &=& \frac{p_{s1}^{cf}}{\rho_{s1}} + \frac{RT}{\hat{m}_{Na}} \ln(x_{NaE}\, x_{ClE}) \\ \mu_{s2E} &=& \frac{p_{s2}^{cf}}{\rho_{s2}} + \frac{RT}{\hat{m}_{Ca}} \ln(x_{CaE}\, x_{ClE}^2)\ , \end{array}\right. \quad \left\{\begin{array}{lcl} \mu_{s1I} &=& \frac{RT}{\hat{m}_{Na}} \ln(x_{NaI}\, x_{ClI}) \\ \mu_{s2I} &=& \frac{RT}{\hat{m}_{Ca}} \ln(x_{CaI}\, x_{ClI}^2)\ , \end{array}\right. \tag{6.4.31}$$

where the salt configurational pressure are defined as :

$$\frac{p_{s1}^{cf}}{\rho_{s1}} = \frac{p_{Na}^{cf}}{\rho_{Na}} + \frac{\hat{m}_{Cl}}{\hat{m}_{Na}} \frac{p_{Cl}^{cf}}{\rho_{Cl}} \quad \text{and} \quad \frac{p_{s2}^{cf}}{\rho_{s2}} = \frac{p_{Ca}^{cf}}{\rho_{Ca}} + 2\frac{\hat{m}_{Cl}}{\hat{m}_{Ca}} \frac{p_{Cl}^{cf}}{\rho_{Cl}}\ . \tag{6.4.32}$$

Finally, the model (6.4.26) and (6.4.30) illustrates the presence of mechano-chemical coupling. On the one hand, the chemical influence on the mechanical behaviour is mainly embodied in the effective pressure term (p^{eff}). On the other side, the mechanical influence on the chemical behaviour is represented by the pressure terms in the chemical potentials.

Steady state problem closure

The steady state problem is totally described when the bath conditions are specified, viz. when the bath pressure and mass contents are given, and when either the displacement or the stress vector is imposed on the boundaries. The chemical potentials of the

bath for the water and for the salts are written as :

$$\begin{aligned} \mu_{wB} &= \frac{p_B}{\rho_w} + \frac{RT}{\hat{m}_w} \ln x_{wB} \\ \mu_{s1B} &= \frac{p_B}{\rho_{s1}} + \frac{RT}{\hat{m}_{Na}} \ln \left(x_{NaB}\, x_{ClB} \right) \\ \mu_{s2B} &= \frac{p_B}{\rho_{s2}} + \frac{RT}{\hat{m}_{Ca}} \ln \left(x_{CaB}\, x_{ClB}^2 \right) \ . \end{aligned} \tag{6.4.33}$$

As the extrafibrillar compartment communicates with the intrafibrillar compartment and the bath, the equilibrium implies the following equations :

$$\left\{ \begin{array}{c} \mu_{wE} = \mu_{wI} \\ \mu_{s1E} = \mu_{s1I} \\ \mu_{s2E} = \mu_{s2I} \ , \end{array} \right. \tag{6.4.34}$$

and

$$\left\{ \begin{array}{c} \mu_{wE} = \mu_{wB} \\ \mu_{s1E} = \mu_{s1B} \\ \mu_{s2E} = \mu_{s2B} \ . \end{array} \right. \tag{6.4.35}$$

These six last equations close up the elastic model at equilibrium. In the dynamic case, the problem will be closed by other equations as it will be illustrated in the next paragraphs.

6.4.2 Transfer in intrafibrillar compartment

The mass transfer law in the intrafibrillar compartment is going to be determined. This law is again provided by the consequences of the second principle of Thermodynamics. We focus on the second inequality of Eq. (6.4.19) rewritten as Eq. (6.4.40), which is here recalled as :

$$\frac{D^s D_2}{Dt} = -\left(\mu_{wI} - \mu_{wE}\right) \frac{D^s m_{wI}}{Dt} - \left(\mu_{s1I} - \mu_{s1E}\right) \frac{D^s m_{NaI}}{Dt} - \left(\mu_{s2I} - \mu_{s2E}\right) \frac{D^s m_{CaI}}{Dt} \geq 0 \tag{6.4.36}$$

A simple way to satisfy the inequality is to define the mass transfer law as :

$$\frac{D^s}{Dt} \left[\begin{array}{c} m_{wI} \\ m_{NaI} \\ m_{CaI} \end{array} \right] = -[T] \left[\begin{array}{c} \mu_{wI} - \mu_{wE} \\ \mu_{s1I} - \mu_{s1E} \\ \mu_{s2I} - \mu_{s2E} \end{array} \right] , \tag{6.4.37}$$

where $[T]$ is a 3×3 (semi-)positive definite symmetric matrix, which is is called the **transfer matrix**. In a first attempt, an uncoupling between the mass transfers is assumed and the transfer matrix is therefore diagonal. Typically, this property implies

that the sole chemical non-equilibrium of water does not directly result in salt transfer. The transfer parameters of $[T]$ involve the characteristic transfer times τ_k of each species. By means of non-dimensionalization, the following relations are indeed obtained :

$$T_k = \frac{\hat{m}_k}{RT}\frac{\rho_k}{\tau_k}, \quad k = w, Na, Ca. \tag{6.4.38}$$

6.4.3 Fluxes and transfer in extrafibrillar compartment

This section again illustrates how the second principle can help in determining thermodynamically correct constitutive equations. The transport laws will be developed and Darcy's, Fick's and Ohm's laws will be recovered.

The third inequality of Eq. (6.4.19) is written as :

$$\frac{D^s D_3}{Dt} = -\sum_{k\in E^{mo}} \nabla\mu_{kE}^{ec} \cdot M_{kE} \geq 0. \tag{6.4.39}$$

A sufficient condition to satisfy this latter inequality is to postulate the existence of a symmetric positive definite matrix $[\kappa]$ of appropriate size[11] such that :

$$\begin{bmatrix} \frac{M_w}{\rho_w} \\ \frac{M_{Na}}{\rho_{Na}} \\ \frac{M_{Ca}}{\rho_{Ca}} \\ \frac{M_{Cl}}{\rho_{Cl}} \end{bmatrix} = \begin{bmatrix} J_w \\ J_{Na} \\ J_{Ca} \\ J_{Cl} \end{bmatrix} = -[\kappa] \begin{bmatrix} \rho_w \nabla\mu_w^{ec} \\ \rho_{Na} \nabla\mu_{Na}^{ec} \\ \rho_{Ca} \nabla\mu_{Ca}^{ec} \\ \rho_{Cl} \nabla\mu_{Cl}^{ec} \end{bmatrix}, \tag{6.4.40}$$

The $[\kappa]$ components can be determined by developing the summation in (6.4.39). The matrix detail can be found in Annexe E. Considering indeed the decomposition of the potential μ_{kK}^{ec} (6.4.17) into (i) a mechanical part, (ii) a chemical part, and (iii) an electrical part, the following inequalities are satisfied :

- $-\sum_{k\in E^{mo}} \nabla p_{kE} \cdot J_{kE} \approx -\nabla p_{wE} \cdot J_{wE} \geq 0$, which means that the flux of water is opposite and proportional to the pressure gradient, thereby providing Darcy's law.
- $-\sum_{k\in E^{mo}} \frac{RT}{\hat{v}_k} \nabla \ln x_{kE} \cdot J_{kE}^d \geq 0$, (where J_{kE}^d is the diffusive flux of the ion k) which means that the diffusive flux of the ion is opposite and proportional to the concentration variation, thereby providing Fick's law.

[11] In 1D, the κ matrix size is 4×4, whereas in 3D 12×12.

- $-I_{eE} \cdot \nabla \phi^E \geq 0$, which means that the electrical current is opposite and proportional to the electrical potential gradient, thereby providing Ohm's law.

The interested reader will find the developments related to these expressions and above all the details of the transport matrix κ in (57).

6.4.4 Closure of the non-equilibrium problem

This section is devoted to show that the closure of the equation set is achieved. In the two last paragraphs, several new unknowns and equations have indeed been added to the global picture.

Table 6.1: Total problem unknowns for two salts and in 3D.

Unknowns	Number
Mass contents : $m_{kK}, k \in E^{mo}, K \in \{I,E\}$	8
Electrochemical potentials : $\mu^{ec}_{kE}, k \in E^{mo}$	4
Chemical potentials : $\mu_{wI}, \mu_{s1I}, \mu_{s2I}$	3
Volumic flux $J_{kE} k \in E^{mo}$	12
Stress tensor components : σ_{ij}	6
Strain tensor components : ε_{ij}	6
Displacement components : u_i	3
Pressure terms : p^{eff}, p_I	2
Hydration term : p^h	1
Electrical potential field : ϕ^E	1
Total	46

Tables 6.1 and 6.2 represent a sketch of the complete problem. The number of independent equations is equal to the number of unknowns. However, at this stage, several remarks remain needed :

- The extrafibrillar **electrochemical** potentials are used in the flux law. In the transfer law, only the intrafibrillar **chemical** potentials are necessary. This shows that the intrafibrillar electrical potential field is not required in order to obtain the global solution and is thus not determined.
- Knowing the mass contents, the molar fractions can be deduced by the relations shown in Section 6.2.3.

Table 6.2: Total problem equations for two salts and in 3D

Equations	Number
Mass conservation (6.3.14)	1
Momentum balance (6.3.15)	3
Phase transfer (6.3.13)	4
Transfer law (6.4.37)	3
Flux law (6.4.40)	12
Definition of the deformation tensor	6
Stress tensor constitutive law (6.4.26)	6
Electrochemical potential constitutive law (6.4.17)	4
Chemical intrafibrillar potential $(6.4.30)_5$ and $(6.4.31)_{3,4}$	3
Hydration pressure (p^h) (6)	1
Effective pressure p^{eff} (6.4.29)	1
Electroneutrality condition (6.2.3)	2
Total	46

- The present problem differs from the previous problem because of its non-stationary and non-homogeneous aspects. The unknowns can vary with position and time. The model is an EDP set and appropriate boundary and initial conditions must be added to complete it. This point will be address at a later stage.

- To analyse this problem we used the finite element method.

6.4.5 Possible improvements of the model

Several effects observed in cartilage behaviour were not accounted for. Most of all the model should consider (i) the anisotropy effects and (ii) the material non-homogeneity.

The elasticity anisotropy is partly taken into account by the elastic cone-behaviour. Nevertheless the collagen fibril behaviour could better be represented by a more elaborate non-isotropic model (typically a transversely isotropic model).

The solid phase (collagen fibril) and the PG contents basically vary with the cartilage depth. This induces that elastic (such as the Young and compressibility moduli) and chemical properties can vary with the location and are then non-homogeneous. Besides, the variation of these properties is dependent of the cartilage origin (animal,

human, ...) and the considered individual.

Finally, as it appears in (6; 57), this model requires several physical parameters which must be determined by means of appropriate experimental results. Unfortunately, this issue remains a very hard task.

6.5 Solution

This section is devoted to present a numerical solution to the previously developed problem (Table 6.2). For the sake of generality, the problem will be considered as tridimensional and with two salts.

A reduced equation set will firstly be presented and justified. The problem discretization will be investigated and a global algorithm will be detailed. Finally, numerical results will be compared with experimental measurements from oedometrical tests.

6.5.1 A reduced equation set

As shown in the previous section, the problem has a very high number of unknowns (46 !) and corresponding equations. Nevertheless as it has been proved by Simões et al. (58), it is possible to isolate a set of primary unknowns (denoted by $\mathbb{X}$) and a related equation set. The other unknowns (or secondary unknowns) can then be determined by a linearization process which includes variations of the (time derivative of the) primary unknowns as based on the remaining equations. The primary unknows are selected in such a way that each species of each phase is represented in this primary set.

Typically in (58), the primary unknowns are :

(i) for the solid phase : the displacement (u),

(ii) for the extrafibrillar phase : the electro-chemical potential of the extrafibrillar species ($\mu^{ec}_{kE}, k \in E$)[12],

(iii) for the intrafibrillar phase : the mass contents of the intrafibrillar species ($m_{kI}, k \in I'$)[13],

[12]The PG influence is taken into account by means of the electroneutrality condition.

[13]The chloride influence is taken into account by means of the electroneutrality condition.

while the equation set is composed of the momentum balance (6.3.15), the total mass conservation equation (6.3.14), the extrafibrillar species mass conservation equation (6.3.13) and the intrafibrillar transfer law (6.4.37).

In order to apply the finite element method the weak formulation of the problem is developed. After multiplying the equations by the related test-functions, the equations are integrated on the studied volume (V) and can be transformed by means of integrations by parts. Denoting the test-functions by $\underline{u}^*$, μ^*, and m^*, respectively, and the integration volume and its boundary by V and ∂V, the weak formulation rewrites as :

$$\begin{aligned}
\int_V \underline{\nabla u}^* : \underline{\sigma}\, dV &= \int_{\partial V} \underline{u}^* \cdot \underline{\sigma} \cdot \underline{n} dS, \\
\int_V \mu^* \underline{\nabla} \cdot \underline{v_s} - \underline{\nabla} \mu^* \cdot \underline{J_E}\, dV &= -\int_{\partial V} \mu^* \underline{J_E} \cdot \underline{n} dS, \\
\int_V \mu^* \left(\frac{D^s v_{kI}}{Dt} + \frac{D^s v_{kE}}{Dt} \right) - \underline{\nabla} \mu^* \cdot \underline{J_{kE}}\, dV &= -\int_{\partial V} \mu^* \underline{J_{kE}} \cdot \underline{n} dS, \quad k \in E^{ions}, \\
\int_V m^* \left(\frac{D^s m_{kI}}{Dt} - T_k \left(\mu_{k'E} - \mu_{k'I} \right) \right) dV &= 0, \quad (k,k') = (w,w), (Na,s_1), (Ca,s_2).
\end{aligned} \tag{6.5.41}$$

The left-hand side is here called the **internal force** ($\mathbb{F}^{int}$) while the right-hand side is called the **external force** ($\mathbb{F}^{ext}$). The previous equation set is then summarized as :

$$\mathbb{F}^{int} = \mathbb{F}^{ext} \ . \tag{6.5.42}$$

To complete this equation set, boundary and initial conditions must be added. The cartilage is bathed in a solution with an electrolyte with a determined molarity, under a determined electrical potential field and with a determined stress/deformation, which means that the electro-chemical potential and the stress/deformation are imposed along the boundaries. The boundary conditions are then :

- force per unit area ($\underline{\sigma} \cdot \underline{n}$) or displacement ($\underline{u}$) imposed on ∂V ;
- electro-chemical potential of extrafibrillar species (μ_{kE}^{ec}) or fluxes imposed on ∂V .

Finally, if the problem starts from an equilibrium state, the initial state is determined by solving the homogeneous-equilibrium problem with specified initial conditions (bath composition, bath pressure and stress or strain).

6.5.2 Solution method

The Newton Raphson method will be applied to problem (6.5.41). This technique consists in finding successive approximations approaching the solution. Typically, considering internal forces depending on $\mathbb{X}$, the final problem (6.5.42) is rewritten as $\mathbb{F}^{int}(\mathbb{X}) = \mathbb{F}^{ext}$. If $\mathbb{X}_i$ denotes the approximation at the i^{th}-iteration, the $\mathbb{X}_i$ increment (denoted by $\Delta\mathbb{X}_i$) is calculated in such a way that $\mathbb{F}^{int}(\mathbb{X}_i) + \Delta\mathbb{F}^{int}_i = \mathbb{F}^{ext}$, where $\Delta\mathbb{F}^{int}_i = \mathbb{K}\Delta\mathbb{X}_i$, with $\mathbb{K} = \frac{d\mathbb{F}^{int}}{d\mathbb{X}}(\mathbb{X}_i)$. Finally the next approximation is defined by the relation $\mathbb{X}_{i+1} = \mathbb{X}_i + \Delta\mathbb{X}_i$.

This method is here applied in an appropriate way to the set of equations (6.5.41). Noting $\underline{u}, (\mu^{ec}_{kE}, k \in E), (m_{kI}, k \in I\backslash\{Cl\})$ by $\mathbb{X}$, it can easily be observed that, on the one hand the internal forces depends on $\mathbb{X}$ and $\dot{\mathbb{X}}$ where a dot denotes material derivative with respect to the solid phase and, on the other hand, the external forces vector $\mathbb{F}^{ext}$ depends on $\mathbb{X}$ and on the surface loadings (denoted by $\mathbb{S}$) (58). Equations (6.5.41) are then summarized as follows :

$$\mathbb{F}^{int}(\dot{\mathbb{X}}, \mathbb{X}) = \mathbb{F}^{ext}(\mathbb{X}, \mathbb{S}). \tag{6.5.43}$$

This equation system is strongly non-linear and coupled. Hence the previous method is applied with appropriate adaptations that take into account the dependence of the internal forces upon $\mathbb{X}$ and its time derivative $\dot{\mathbb{X}}$. This latter is chosen as the real primary variable and is integrated versus time to find $\mathbb{X}$. Time integration is performed by means of the implicit Euler method[14].

At the i^{th}-iteration at time t_n, the integration scheme for $\dot{\mathbb{X}}$ (which provides $\mathbb{X}$) is then given by :

$$\text{for } i \geq 1 \ : \begin{cases} \dot{\mathbb{X}}_{i,n} = \dot{\mathbb{X}}_{i-1,n} + \Delta\dot{\mathbb{X}}_{i-1,n} \\ \mathbb{X}_{i,n} = \mathbb{X}_{n-1} + \Delta t_n \, \dot{\mathbb{X}}_{i,n} = \mathbb{X}_{i-1,n} + \Delta\dot{\mathbb{X}}_{i-1,n}\Delta t_n = \mathbb{X}_{i-1,n} + \Delta\mathbb{X}_{i-1,n}, \end{cases} \tag{6.5.44}$$

$\mathbb{X}_{n-1}$ being the converged solution at time t_{n-1}, while the initialization at time t_n is given by :

$$\begin{cases} \dot{\mathbb{X}}_{0,n} = \dot{\mathbb{X}}_{n-1} \\ \mathbb{X}_{0,n} = \mathbb{X}_{n-1} + \Delta t_n \, \dot{\mathbb{X}}_{0,n} = \mathbb{X}_{n-1} + \Delta t_n \, \dot{\mathbb{X}}_{n-1}, \end{cases} \tag{6.5.45}$$

$\dot{\mathbb{X}}_{n-1}$ being the converged solution at time t_{n-1}.

The variation of internal forces during a small time interval results from the variations

[14] As the small displacement hypothesis is applied, the material derivative is the same as the partial time derivative.

of $\dot{\mathbb{X}}$ and of $\mathbb{X}$. Defining

$$\mathbb{K} = \frac{\partial \mathbb{F}^{int}}{\partial \mathbb{X}} \quad \text{and} \quad \mathbb{C} = \frac{\partial \mathbb{F}^{int}}{\partial \dot{\mathbb{X}}} \,, \tag{6.5.46}$$

this internal force variation hence writes as :

$$\Delta \mathbb{F}^{int} = \mathbb{C}\, \Delta \dot{\mathbb{X}} + \mathbb{K}\, \Delta \mathbb{X}. \tag{6.5.47}$$

The variation of $\dot{\mathbb{X}}$ is calculated in such a way that the internal force is closer and closer to the external force. At the i^{th}-iteration associated with time t_n, the previous considerations provide the way to determine the appropriate $\Delta \dot{\mathbb{X}}_{i-1,n}$ increment. Indeed, the following relations are successively found :

$$\begin{array}{lcl} \mathbb{F}^{int}_{i-1,n} + \Delta \mathbb{F}^{int}_{i,n} & = & \\ \mathbb{F}^{int}_{i-1,n} + \mathbb{C}_{i-1,n} \Delta \dot{\mathbb{X}}_{i,n} + \mathbb{K}_{i-1,n}\, \Delta \mathbb{X}_{i-1,n} & = & \\ \mathbb{F}^{int}_{i-1,n} + (\mathbb{C}_{i-1,n} + \mathbb{K}_{i-1,n}\, \Delta t_n)\, \Delta \dot{\mathbb{X}}_{i-1,n} & = & \mathbb{F}^{ext}_{i-1,n} \end{array} \tag{6.5.48}$$

The secondary variables are updated at each iteration by the simple linearization process described in (57) and (58), in order to take into account the unconsidered equations.

6.5.3 FEM method

In order to determine $\Delta \dot{\mathbb{X}}_{i-1,n}$ at every iteration i of each time step, the adaptation of the formulation (6.5.48) shows that the following linear system must be solved :

$$(\mathbb{C}_{i-1,n} + \mathbb{K}_{i-1,n}\, \Delta t_n) \Delta \dot{\mathbb{X}}_{i-1,n} = \mathbb{F}^{ext}_{i-1,n} - \mathbb{F}^{int}_{i-1,n} \tag{6.5.49}$$

Let us recall that the primary variable is $\dot{\mathbb{X}}$, as representing the time derivative of the displacement (1), of the electro-chemical potentials (4), and of the intrafibrillar mass contents (3). For a 1D problem, there are 8 unknowns per nodes. As it is usual in elasticity, quadratic polynomial functions are chosen in order to interpolate the displacement while linear polynomials are selected for the other variables. In conclusion, it appears that the system (6.5.49) essentially results from the linearization process and from algebraic manipulations on the weak formulation (6.5.41).

6.5.4 Numerical results on oedometrical test

The oedometrical test consists in imposing a confined compression on a material sample (Fig. 6.5).

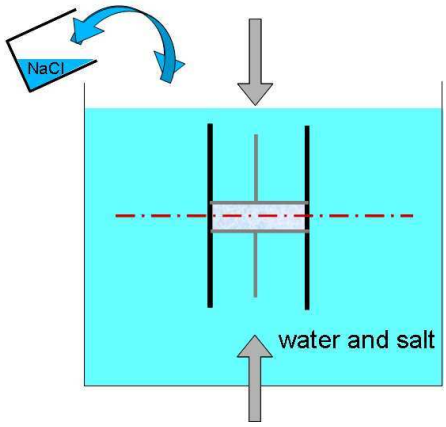

Figure 6.5: Oedometrical test with variation of the bath salinity.

In the present case, the material is cartilage and is in contact with a bath whose salt concentration can be changed. Eisenberg and Grodzinsky (7) relate oedometrical experiments performed on cartilage. The related measurements are carried out while changing the bath salinity (NaCl) and can be summarized in a strain-stress diagram Fig. 6.6 , which is drawn when equilibrium is reached at each step of the process.

We here show numerical results from a 4-operation cycle computed with our program. Beginning with a stress-free 1M bathed sample, the cartilage sample successively undergoes four sollications, viz. :

1. a NaCl bath molarity change from 1M to 0.01M while the displacement of the sample extremities is imposed to be zero ;
2. an imposed displacement of the extremities at $-5.25\ 10^{-4}$m while the NaCl bath molarity is maintained at 0.01M ;
3. a NaCl bath molarity change from 0.01M to 0.1M under constant strain ;
4. an imposed displacement of the extremities at $-3.75\ 10^{-4}$m while the NaCl bath molarity is maintained at 0.1M.

The changes are performed during a 120 s period before waiting during 3 h for reaching stabilization. Fig. 6.6 give experimental results performed on a 0.6 mm depth cartilage sample, showing the evolution of the total stress as a function of the deformation

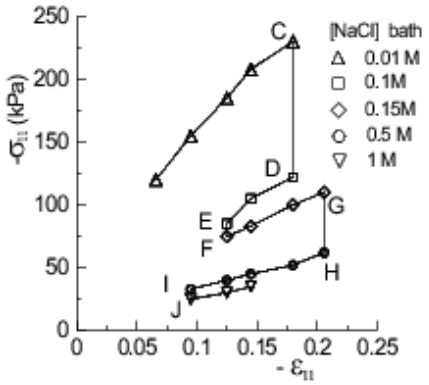

Figure 6.6: Experimental measurements at equilibrium from oedometrical tests (7) .

at equilibrium. These measurements can be compared to the numerical results of Fig. 6.7 whose parameter values can be found in the Annexe F. Good agreement is observed between the measurements and the model at equilibrium and this leads us to plot different fields and to compare the effect of some physical parameters.

First of all, let us show numerical results relating the evolution of mass contents, extrafibrillar electrical potential and pressure p_I as a function of time and position during the different steps of the experiments (Figs. 6.8-6.13). Since in the study of clays it is observed that the sodium characteristic transfer time is much higher than the water characteristic transfer time (Eq. (6.4.38)) (61), we have firstly investigated the cases where $\tau_{Na} = 15.5\ 10^4$ s and $\tau_w = 7.4$ s. Numerical results were performed by means of a 30 element mesh where only half of the sample was considered because of the problem symmetry.

Typically, it is observed that when the salinity is decreased (first step), there is a depletion of intrafibrillar water (Fig. 6.9) whereas the extrafibrillar mass content increases (Fig. 6.8). In compression (second step), both compartments expel water (Fig. 6.8 and 6.9).

For the sodium mass content, we notice during the first step the non-mobile ions are present in the extrafibrillar phase (Fig. 6.10). Indeed, even if the salt molarity is nearly close to zero, because of the PG presence combined with the electroneutrality condition, there is a non-negligible sodium amount in opposition to what is observed in the intrafibrillar compartment (Fig. 6.11).

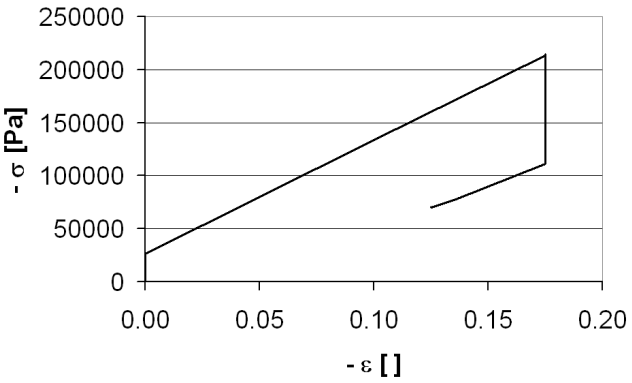

Figure 6.7: Numerical results from oedometrical tests. Normal stress versus longitudinal deformation in the 4-step cycle.

Secondly, as this model is the first model with two compartments, it is important to quantify the mass transfer between these compartments. In order to address this issue, we analyse the effect of the most significant paremeter on this phenomenum, viz. the characteristic transfer time. We have thus computed the solution for other characteristic times, viz. $\tau_{Na} = 15.5\ 10^6$s and $\tau_w = 7.4$s in order to compare the transient results with future experimental results. Steady state values are unaffected by transfer times, since the material behaviour is not path-dependent. Nevertheless as shown on figures 6.14 and 6.15 , steady state requires more time to get established with these new parameters.

Let us consider the stage 1 where the chemistry is refreshed at constant strain. For the smaller transfer time, intrafibrillar sodium ions are extracted more quickly (Fig. 6.15 (a) and (b)), and therefore the amount of extrafibrillar sodium ions is larger at any time (Fig. 6.14 (a) and (b)). These extrafibrillar ions leave the specimen by diffusion. At time 30 s, the information has reached the bottom of the mesh (here not shown). Their spatial profile is monotonous, as is the profile of the intrafibrillar sodium ions whose changes depend much on the transfer time.

For larger transfer time of Na^+, the amount of extrafibrillar Na^+ is smaller (time 480 s on Fig. 6.14 (a) and (b)), because the Na^+ initially in the EFC can diffuse, and diffusion is almost complete when the intrafibrillar ions are able to penetrate the EFC, from where they are expelled by diffusion (Figs. 6.14 and 6.15).

For the water mass content evolution, the transient phenomena are very strong, as it is shown by the time and space evolutions (Fig. 6.14). It can be observed that there is a competition between diffusion (that dominates initially) and electro-mechanics (that dominates in later times) that dictates contradictory trends.

Indeed, initially, diffusion dominates the extrafibrillar compartment, and it tends to expel water according to the osmotic effect, since ions leave the cartilage as the bath is refreshed. Nevertheless, since the height of the specimen is imposed, water cannot really leave the sample, and it enters the IFC. At subsequent times, there is a competition betwen diffusion that dominates longer in the lower part of the mesh, and electro-mechanics that tends to get established initially at the top of the mesh, where the displacement is controlled. So, with time, electro-mechanics penetrates the specimen downward. Electro-mechanics manifests itself by the fact, that, since cations leave the EFC, the repulsion between the PG's is larger, and water has to enter this compartment. This water comes in fact from the IFC where it was pushed in a first time by diffusion (Fig. 6.14).

If the transfer time of ions is increased, then the diffusion phenomenon is increased for the water mass contents, because there are less ions in the EFC, and thus need less water according to the osmotic phenomenon. Thus, the decrease in EF water and increase in IF water is larger, and the time to reach steady state longer as well, because electro-mechanics will have a more adverse situation to reverse than in previous case(Fig. 6.14).

6.6 Conclusions

This model is the first model with two fluid compartments and we were able to numerically analyze the effect of the characteristic time on the mass tranfer between the two concerned compartments.

Even if the last results are satisfactory, our model and numerical solution should be improved.

First of all, the calibration of the model parameters is a difficult task. These parameters are indeed numerous since the nature of the physiological tissue involves a lot of physical and chemical phenomena which are usually complicated to model. Nevertheless, we want to keep the model as complete as possible and therefore several parameters must be adjusted.

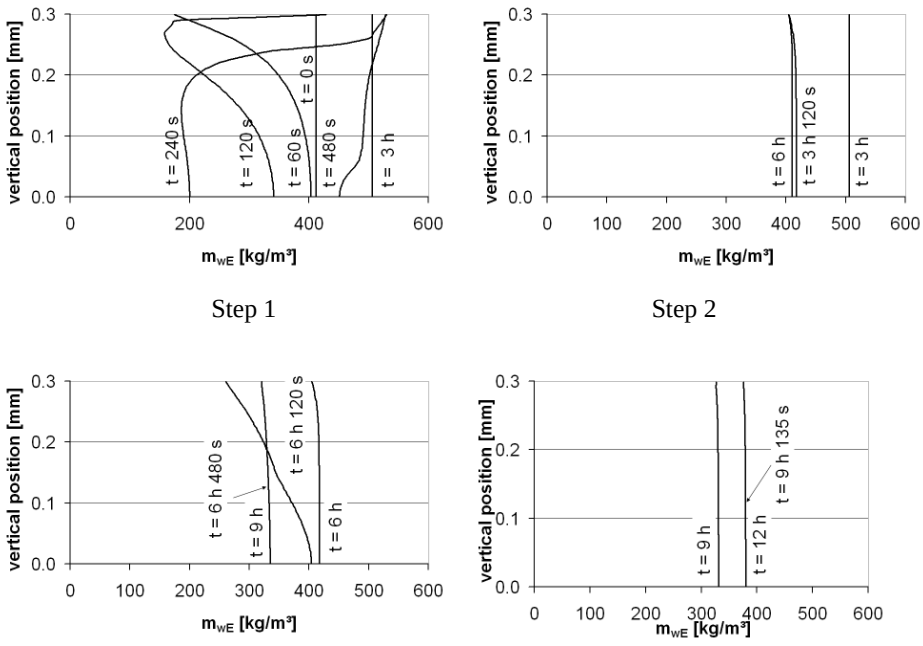

Figure 6.8: Numerical results from oedometrical tests. Evolution in time and space of the extrafibrillar water mass content during the 4 steps of the cycle with $\tau_{Na} = 15.5\ 10^4$ s, $\tau_w = 7.4$ s.

Moreover, even if experimental measurements are described in the literature, these data are usually not complete to determine all the system parameters and to entirely build the model.

Finally, the model induces some numerical difficulties. For example, reaching pure water state (as in distilled water) is easily performed in the experiments. However, as a logarithmic term appears in the model equations, this state is more difficult to approach numerically. Other difficulties of the same type (such as the presence of hyperbolic functions in the interpolation form of p^h) must also be taken into account in order to model the missing constitutive equations (p^h, p_0^{eff}). Moreover, both the linearization process and the primary variable set are not unique.

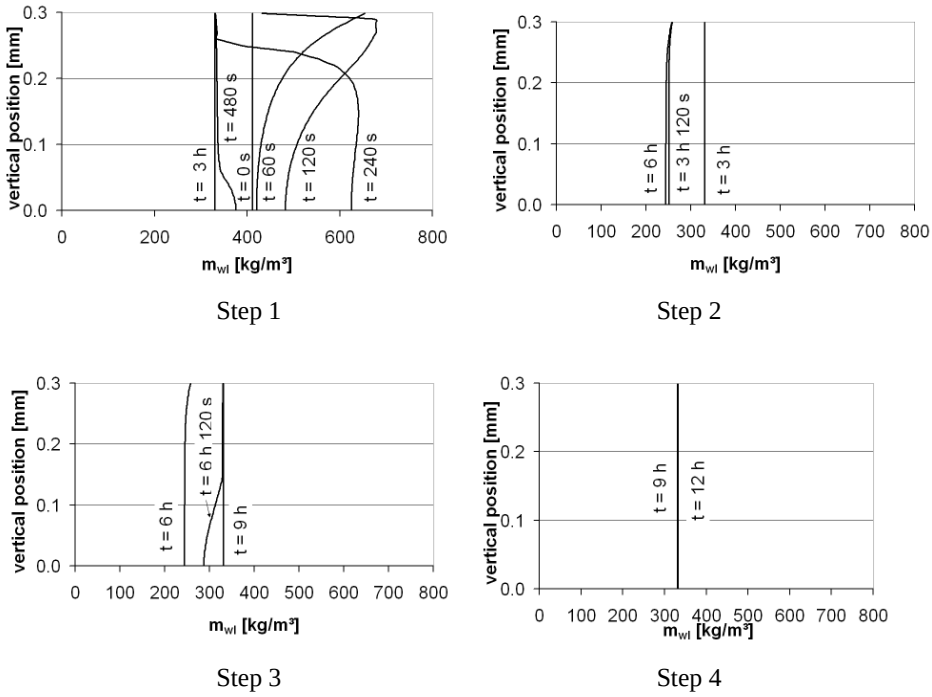

Figure 6.9: Numerical results from oedometrical tests. Evolution in time and space of the intrafibrillar water mass content during the 4 steps of the cycle with $\tau_{Na} = 15.5\ 10^4$ s, $\tau_w = 7.4$ s.

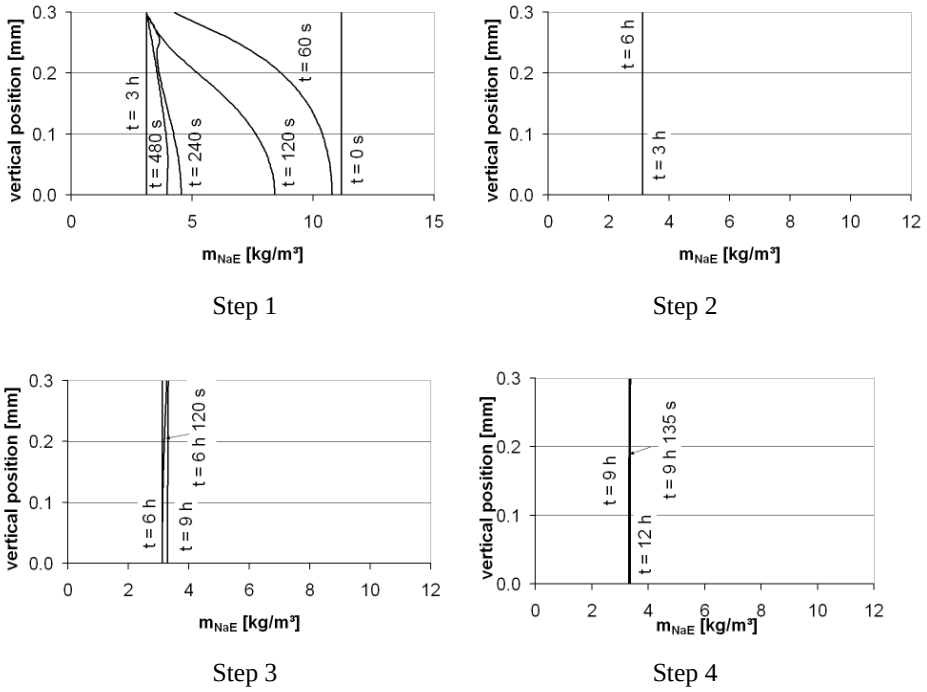

Figure 6.10: Numerical results from oedometrical tests. Evolution in time and space of the extrafibrillar sodium mass content during the 4 steps of the cycle with $\tau_{Na} = 15.5\ 10^4$ s, $\tau_w = 7.4$ s.

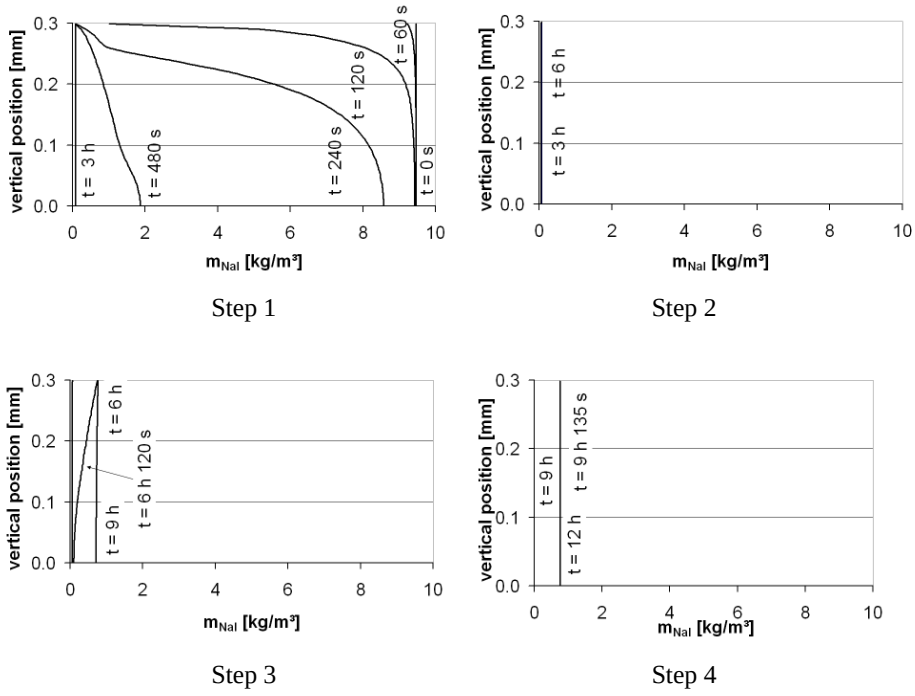

Step 1 Step 2

Step 3 Step 4

Figure 6.11: Numerical results from oedometrical tests. Evolution in time and space of the intrafibrillar sodium mass content during the 4 steps of the cycle with $\tau_{Na} = 15.5\ 10^4$ s, $\tau_w = 7.4$ s.

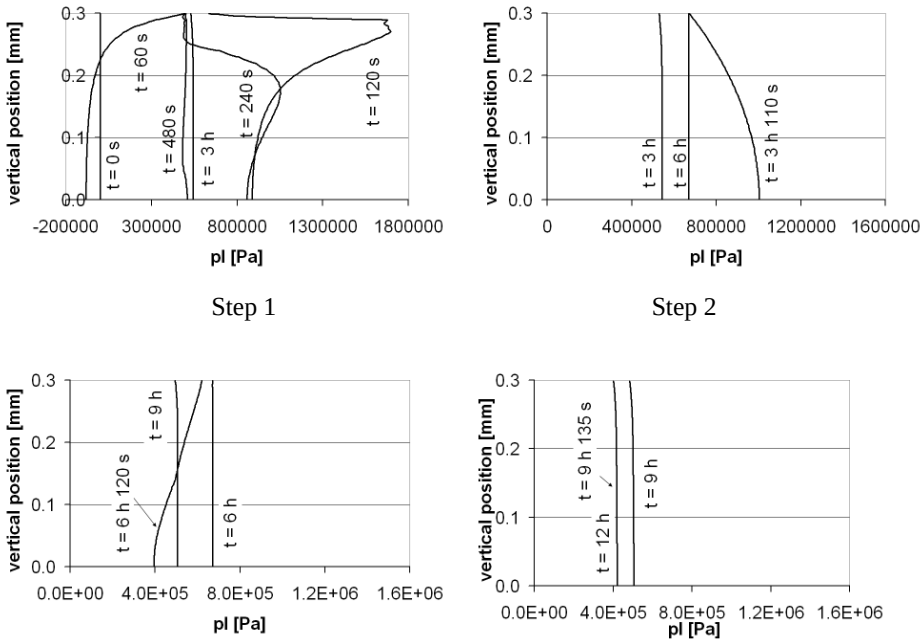

Figure 6.12: Numerical results from oedometrical tests. Evolution in time and space of the pressure p_I during the 4 steps of the cycle with $\tau_{Na} = 15.5\ 10^4$ s, $\tau_w = 7.4$ s.

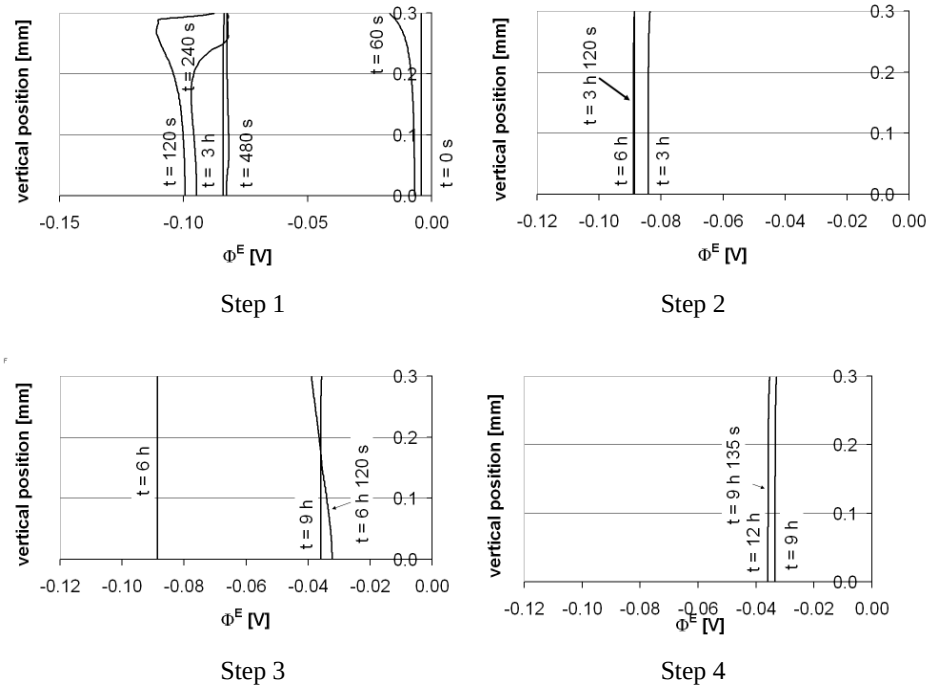

Figure 6.13: Numerical results from oedometrical tests. Evolution in time and space of the electrical potential field during the 4 steps of the cycle with $\tau_{Na} = 15.5\ 10^4$ s, $\tau_w = 7.4$ s.

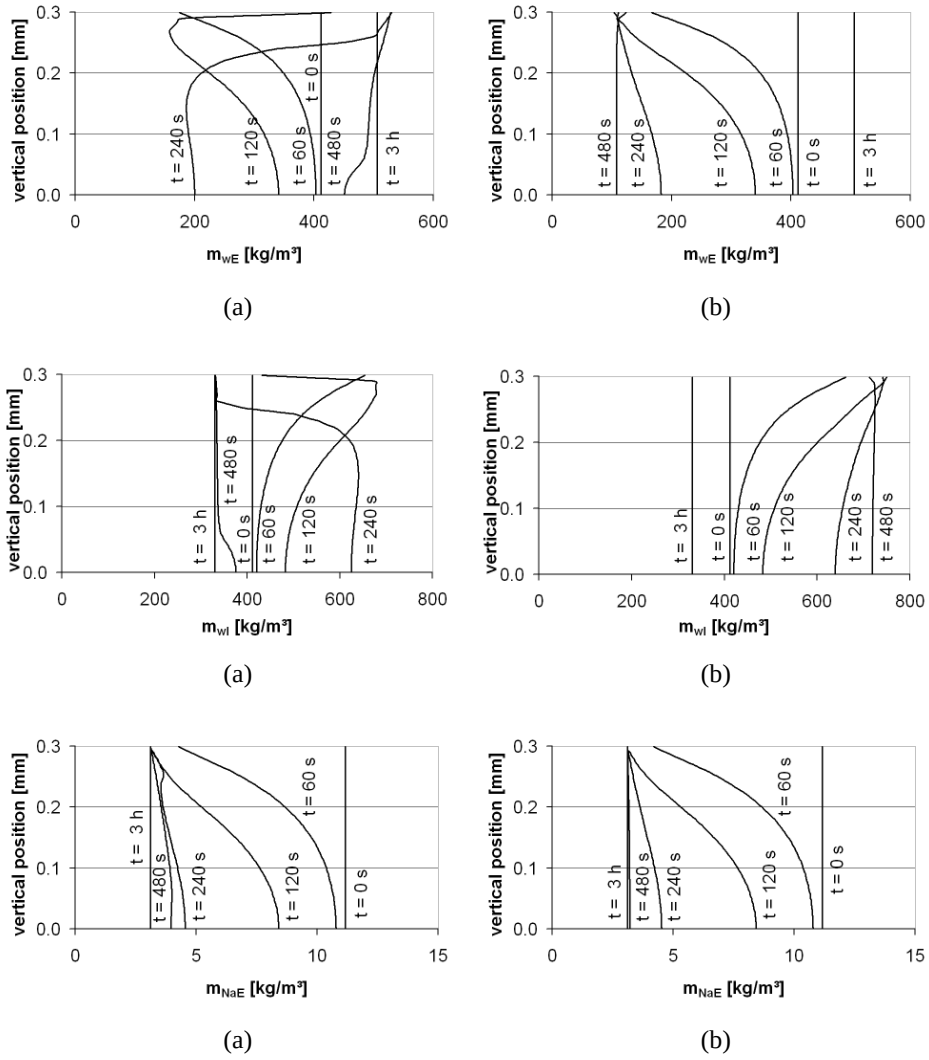

Figure 6.14: Numerical results from oedometrical tests. Comparison of the evolution in space and time of the water and EFC sodium mass contents during the first step of the cycle with different characteristic time scales : (a) $\tau_{Na} = 15.5\ 10^4$ s, $\tau_w = 7.4$ s and (b) $\tau_{Na} = 15.5\ 10^6$ s, $\tau_w = 7.4$ s.

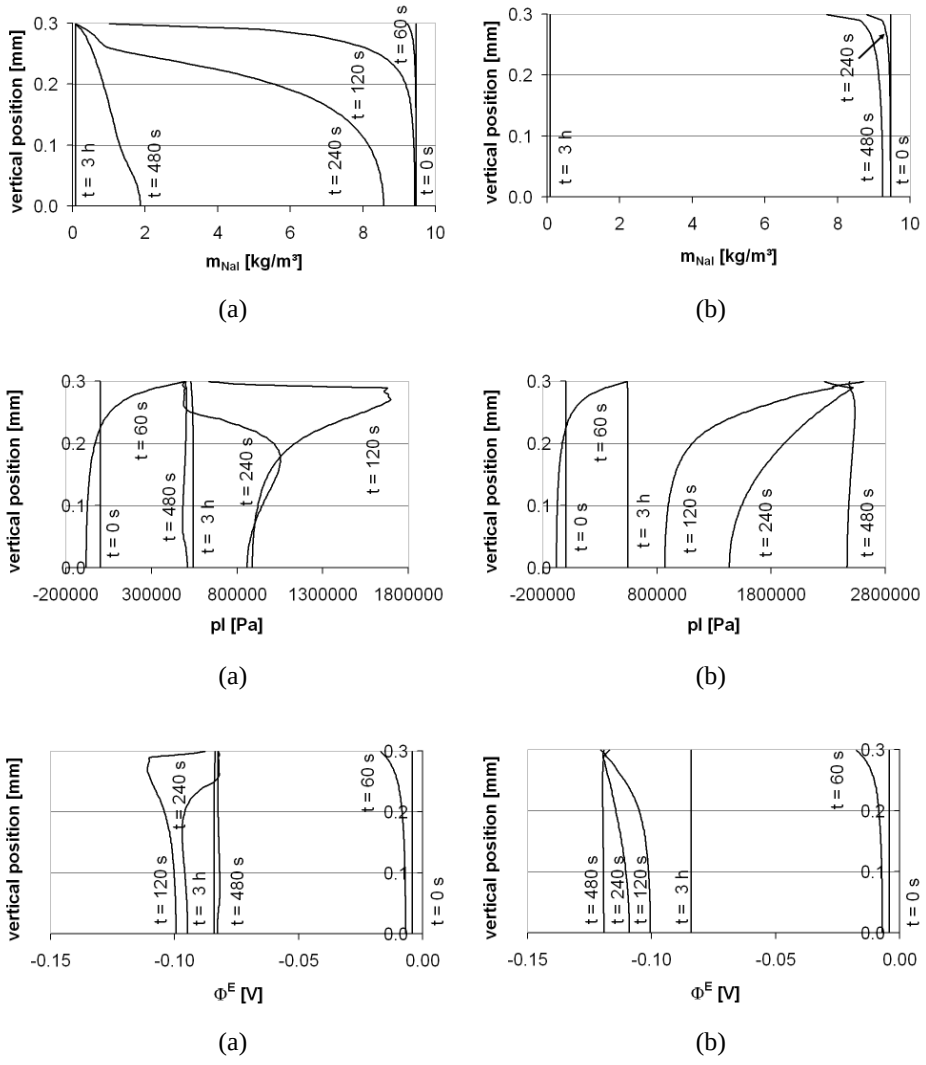

Figure 6.15: Numerical results from oedometrical tests. Comparison of the evolution in space and time of the IFC sodium mass content, of the pressure p_I and of the electrical potential during the first step of the cycle with different characteristic time scales : (a) $\tau_{Na} = 15.5\ 10^4$ s, $\tau_w = 7.4$ s and (b) $\tau_{Na} = 15.5\ 10^6$ s, $\tau_w = 7.4$ s.